Desalination and Water Treatment
www.deswater.com
doi: 10.1080/19443994.2015.1015306

57 (2016) 230–237
January

Taylor & Francis
Taylor & Francis Group

Efficient removal of azo dye by grated copra biomass

Khanom Simarani*, Muhammad Naziz Saat, Mohamad Suffian Mohamad Annuar

Faculty of Science, Institute of Biological Sciences, University of Malaya, 50603 Kuala Lumpur, Malaysia, Tel. +603 7967 5843; Fax: +603 7967 4178; emails: hanomks@gmail.com, hanom_ss@um.edu.my (K. Simarani)

Received 5 October 2014; Accepted 23 January 2015

ABSTRACT

This paper reports on a study showing the feasibility and potential of grated copra biomass (GCB) as natural biosorbent for removal of methylene blue (MB) dye from aqueous solution. The factorial design analysis was applied to screen the effects of biomass dosage and initial dye concentration on the adsorption of MB. About 0.75 g biomass was found to be the most optimum biomass for decolorization resulting in 80–85% dye decolorization for initial dye concentration ranging from 2 to 8 μg mL^{-1}. Freundlich adsorption isotherm satisfactorily explained the kinetics of the dye removal. The porous microstructure of the copra biomass allows for the penetration of its surface during dye adsorption. The removal of dye contaminant by GCB from water bodies is potentially low-cost and environmentally friendly technology.

Keywords: Grated copra biomass; Freundlich isotherm; Adsorption; Methylene blue dye removal; Degradation

1. Introduction

Dyes are highly colored molecules with low biodegradability [1] and almost every industry, e.g. textiles, printing, dye synthesis, leather, pulp mills, food production, and plastic production, use chromophoric materials to give color to their products [1,2]. Most dyes are low in biodegradability due to their complex aromatic molecular structures which are usually a stable compound [3]. There are more than 100,000 types of dyes with over 700,000 tonnes of dyed products produced yearly. These dyes can be classified as either anionic or cationic according to their structure [4]. Given the massive amount of dyes used and colored products produced, the discharge of colored effluents especially from industrial wastewater into water bodies, such as rivers and streams, constitute one of the major sources of water pollution [5]. Due to its color, the presence of dye in water makes it the most easily recognizable pollutant even though it is present in minimum quantities, allowing it to be recognized as aesthetic pollutants [1]. Since these dyes are recalcitrant compounds due to their stability to light and oxidation, they posed strong challenges for conventional treatment methods such as aerobic digestion [5].

Various treatment methods have been developed for the removal of heavy metals and colored substances in water, such as coagulation using alum, lime, ferric chloride, and ferric sulfate; chemical oxidation

---

*Corresponding author.

Presented at the International Conference on Business, Economics, Energy and Environmental Sciences (ICBEEES) 19–21 September 2014, Kuala Lumpur, Malaysia

methods using chlorine and ozone; membrane separation and electrochemical processes [1,2,6]. However, these treatments were highly time consuming, expensive and may lead to other contaminations [7]. The biosorption technique is proposed as an effective and economical treatment method as compared to the currently applied methods mentioned earlier [1,2]. Activated carbon is an example of biosorbent which has many applications as an efficient and versatile adsorbent for water treatment [2]. Due to the operating cost of water treatment using activated carbon is high, attention to the use of unconventional biosorbents in water treatment is very important as an alternative technique.

Agricultural wastes have drawn research interests in their utilization as non-conventional biosorbents [8]. Dual benefits can be fulfilled by the utilization of these agro-wastes in wastewater treatment *viz.* converting wastes into useful materials and, at the same time, it saves waste disposal costs and prevents the on-site burning of these wastes [8]. The coconut is an important crop for the people in the Asia Pacific region, especially in small- and medium-scale economy and to some, for their cultural practices. Grated copra biomass (GCB) is the agro-industrial waste left behind after fresh coconut meat was ground and then pressed to extract the milk. GCB is commonly utilized as feed for livestock, including chickens and swine [9]. GCB has also been traditionally used for cleaning and polishing surfaces such as floors and walls. Unlike the other coconut biomass such as coconut husk, the utilization of GCB in wastewater treatment, however, has not been fully explored.

Thus, the objective of this study was to determine the ability and potential of GCB as an alternative and viable natural biosorbent for dye removal in wastewater treatment. The investigation was carried out on the effect of selected treatment parameters i.e. biomass dosage initial dye concentration on the adsorption of methylene blue (MB) by using statistical experimental design. The kinetics of the adsorption were examined using the Langmuir and Freundlich isotherms.

2. Materials and methods

2.1. Preparation of GCB

The GCB sample was collected from a coconut milk vendor from a local market and washed thoroughly prior to oven dried at 50˚C for 24 h. The dried GCB was then blended using a commercial blender (Phillips HR2001). The fine fibers were then stored at room temperature (25 ± 1˚C) in a sealed airtight container until it was ready to be used. The proximate analysis was performed using the standard methods described in the AOAC protocol [10].

2.2. Preparation of MB dye stock solution

The MB stock solution (1 mg mL^{-1}) was prepared by dissolving of 1 g of MB powder (BDH Chemicals) into 1 L of distilled water. The stock solution was stored at room temperature and was further diluted to desired concentrations.

2.3. Estimation of percentage of decolorization

Samples from the solution's upper layer was obtained at every sampling time and centrifuged at 10,000 rpm for 3 min to sediment any suspended GCB and debris prior to spectrophotometric analysis. The absorbance of the supernatant was measured at 664 nm (optimum wavelength of MB absorption obtained from spectrum analysis). The residual dye concentration in the supernatant was determined by extrapolating the OD value with the MB standard calibration. The percentage of dye decolorization (%) was calculated using the equation as shown below:

$$(\%)\,Decolorization = \frac{OD_0 - OD_t}{OD_0} \times 100 \tag{1}$$

where OD_0 is the initial dye concentration, OD_t is the dye concentration after predetermined in incubation time.

2.4. Full factorial design screening

The effect of GCB weight and initial dye concentration on percentage of decolorization was investigated using design of experiment (DOE). A full factorial design with two levels was used to screen these variables. The minimum and maximum value for the biomass and initial dye concentration is shown in Table 1. Decolorization experiments were done in triplicates according to the design matrix generated by

Table 1
Minimum and maximum value of GCB and initial dye concentration

	Value	
Parameters	Minimum (−1)	Maximum (+1)
GCB (g)	0.5	2.0
Initial dye (μg mL^{-1})	2.0	8.0

GCB: Grated copra biomass.

Minitab 16.0 software (Table 2). The experiments were carried out in 50 mL of dye solution at (25 ± 1℃) for 24 h. Percentage decolorization (%) after 24 h incubation was used as a response for the factorial analysis.

2.5. Kinetic adsorption studies

The kinetic adsorption studies of MB removal were carried out by using 2.25 g of absorbent (GCB) into 250 mL Erlenmeyer flask containing 150 mL of different initial dye concentrations (in mg L^{-1}): 0.5, 1.0, 2.0, 3.0, 4.0, and 5.0. The condition for decolorization experiments was performed using orbital shaker with agitation fixed at 150 rpm and controlled temperature of 25 ± 2℃. The amount of absorbed dye on the GCB (C_a, mg g^{-1}) equilibrium was determined from the equation:

$$q_e = \frac{(C_0 - C_e)V}{M} \tag{2}$$

where V is the volume dye solution (L) and M is the mass of dry GCB absorbent used (g), C_0 and C_e are the initial dye concentration (mg L^{-1}) and dye concentration at equilibrium (mg L^{-1}), respectively.

According to the Langmuir isotherm model, the amount of dye absorbed onto adsorbent (q_e) at equilibrium can be calculated as follows:

$$q_e = \frac{Q_M(K_L C_e)}{1 + (K_L C_e)} \tag{3}$$

where q_e is the amount of absorbed dye of absorbent at equilibrium (mg g^{-1}); C_e is the amount of dye in the liquid phase at equilibrium (mg L^{-1}), K_L is the Langmuir constant being related to the free energy of adsorption (L mg^{-1}), and Q_m is the maximum absorbed dye per unit mass of adsorbent at the monolayer sites of the surface (mg g^{-1}). The model assumes a monolayer adsorption of the adsorbed solute [11].

Another established model describing the adsorption capacity of dye onto solid absorbent is Freundlich isotherm model. The model assumes heterogeneous adsorption due to the diversity of adsorption sites. In this case, the adsorbed dye on the surface of adsorbent resulted in the multilayer adsorption. The equation describing Freundlich isotherm for the amount of dye absorbed onto adsorbent is:

$$q_e = K_F(C_e)^{1/n} \tag{4}$$

where K_F and n are the Freundlich constants related to the adsorption capacity for multilayer adsorption sites (L mg^{-1}) and the dimensionless number of adsorption intensity, respectively.

2.6. Scanning electron microscopy (SEM)

The surface morphology of GCB was observed under scanning electron microscope (Philips Scanning Electron Microscope 515) before and after adsorption of the dye.

Table 2
Design matrix for two-level full factorial design and the experimental and predicted values for the percentage decolorization

	Coded level		Actual concentration		Response	
Experimental order	GCB	Initial dye	GCB (g)	Initial dye (μg mL^{-1})	Experimental	Predicted
1	−1	−1	0.5	2.0	84.2	83.4
2	+1	+1	2.0	8.0	84.7	86.3
3	+1	+1	2.0	8.0	88.7	86.3
4	−1	+1	0.5	8.0	79.9	80.3
5	−1	+1	0.5	8.0	80.4	80.3
6	+1	+1	2.0	8.0	85.6	86.3
7	−1	−1	0.5	2.0	83.7	83.4
8	−1	−1	0.5	2.0	82.4	83.4
9	+1	−1	2.0	2.0	63.6	62.9
10	−1	+1	0.5	8.0	80.6	80.3
11	+1	−1	2.0	2.0	61.0	62.9
12	+1	−1	2.0	2.0	64.1	62.9

GCB: Grated copra biomass.
Notes: −1: minimum value.
+1: maximum value.

3. Results and discussion

3.1. The effect of GCB mass and initial dye concentration

The effect of GCB mass and initial dye concentration was screened using full factorial design. The percentage of experimental and predicted decolorization for each experimental run is shown in Table 2. The predicted values of percentage decolorization were determined using the Minitab 16.0. The highest decolorization was observed at GCB and initial MB concentration of 2 g and 8.0 µg mL^{-1}, respectively, with an average percentage of decolorization at 86.3 ± 2.1%. The lowest decolorization (62.9%) was recorded when 2.0 g of GCB and 2.0 µg mL^{-1} of initial dye concentration were used.

To determine the normal distribution probability, residual analysis was performed (Fig. 1). The residuals (experimental value minus the predicted value) obtained did not show significant deviations from normal distribution following the analysis of normality plot (Fig. 1(a)) and the histogram (Fig. 1(c)). The residual data fell very close to the percentage line in the normality plot, and the histogram showed a visibly clear bell-shaped pattern of normal distribution. The variance in experimental data (Fig. 1(b)) was observed to be well within the acceptable −2 and +2 range. Based on Fig. 1(d), the residuals as a function of the experimental order did not show any systematic pattern. Thus, the random order in which the experiments were performed to exclude the possibility of committing systematic errors.

From the analysis of variance (ANOVA) in Table 3, it was found that at $p = 0.05$, the main effects of GCB weight and initial dye concentration toward the percentage of decolorization were significant. In addition, the interaction between biomass dosage and initial dye concentration toward the percentage of decolorization was also significant. Descriptive statistic of the factorial model indicated a good correlation of experimental data toward predicting model with R^2 and R^2 adjusted values of 0.9836 and 0.9775, respectively.

Based on the interaction plot (Fig. 2), the mean response (dye decolorization percentage) increased with the initial dye concentration at the highest setting of GCB dosage. However, the mean response remained almost constant at the lowest setting of GCB (0.5 g) as initial dye concentration was increased from low to high level. This indicated that the active adsorption centers might be saturated at 0.5 g GCB under the conditions applied in the study.

Similar finding was reported in studies using lotus leaf where the percentage of adsorbed MB increased with the concentration of the lotus leaf. This increase, however, was only up to a certain point until no further increase in the removal percentage of dye was observed [4]. Table 4 shows the composition of

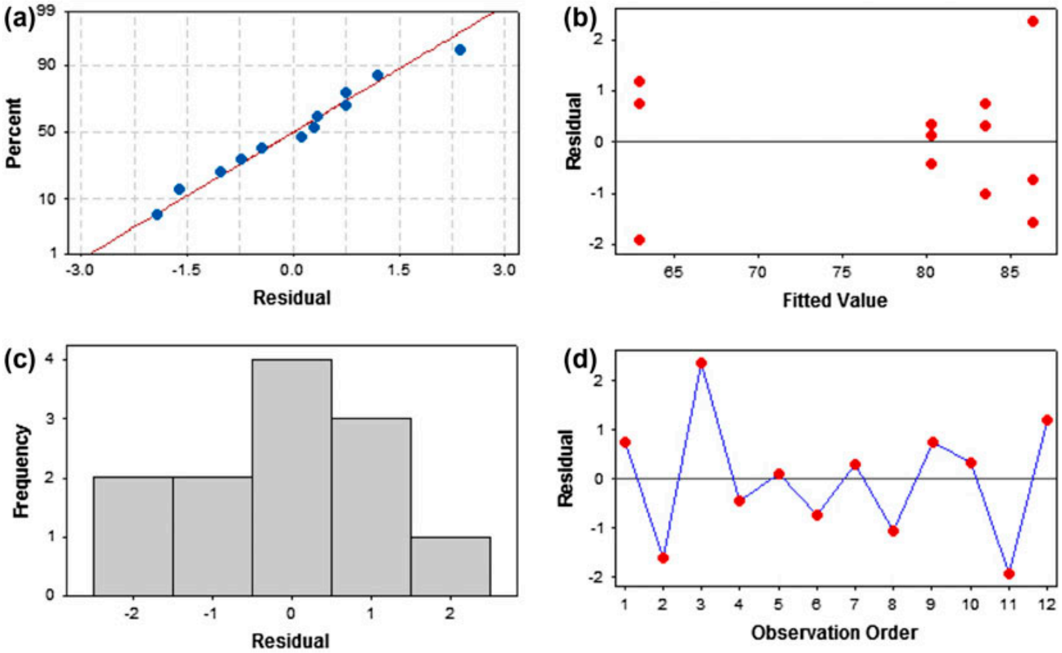

Fig. 1. Residual plot analysis on two-level full factorial design screening on grated coconut biomass weight and initial dye concentration on percentage of decolorization: (a) normal probability plot; (b) residual vs. fitted plot; (c) histogram; and (d) residual vs. observation orders (volume of dye solution = 50 mL, temperature = 25 ± 1˚C, and contact time = 24 h).

Table 3
Analysis of variance for percentage dye decolorization

Source	DF	Seq SS	Adj SS	Adj MS	*F*	*P*
Main Effects	2	466.99	466.99	233.494	112.78	0
Biomass	1	158.63	158.63	158.631	76.62	0
Initial Dye	1	308.36	308.36	308.357	148.94	0
Two-Way Interactions	1	528.94	528.94	528.942	255.49	0
Biomass*Initial Dye	1	528.94	528.94	528.942	255.49	0
Residual Error	8	16.56	16.56	2.07		
Pure Error	8	16.56	16.56	2.07		
Total	11	1,012.49				

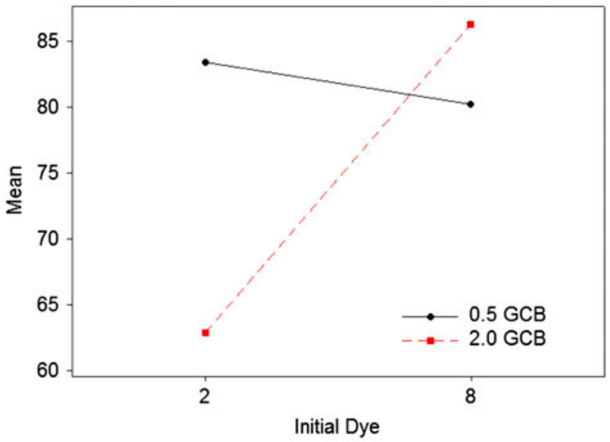

Fig. 2. Interaction of initial dye concentration vs. GCB against percentage of dye decolorization.

lignocellulosic materials, crude protein, and lipid in GCB that may contain active functional groups responsible for the biosorption process. The large surface area to volume ratio of GCB could have arisen from the micropores and mesopores yielding the high porosity nature of the material.

The contour plot (Fig. 3) was constructed to determine extent of interaction between GCB weight and initial dye concentration and to indicate the optimal trajectory of biomass dosage and initial dye concentration.

Table 4
Proximate analysis of GCB

Analysis	Percentage (%)
Lignin	6.53 ± 0.25
Cellulose	45.54 ± 0.04
Hemicellulose	23.78 ± 0.90
Ash	1.10 ± 0.00
Crude protein	4.15 ± 0.12
Oil and Fats	16.87 ± 0.05

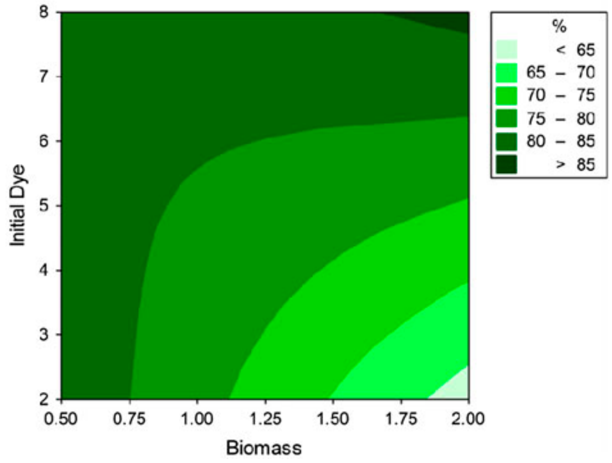

Fig. 3. Contour plot of GCB amount and initial dye concentration against percentage of dye decolorization (volume of dye solution = 50 mL, temperature = 25 ± 1˚C, and contact time = 24 h).

From the contour plot, 0.75 g biomass was predicted to be the most optimum biomass for decolorization because it is expected to result in 80–85% dye decolorization for any initial dye concentration ranging from 2 to 8 μg mL^{-1}. The increases in initial dye concentration lead to decreased dye removal efficiency as well as the increase in the amount of time taken for the system to reach equilibrium [1,2,5].

3.2. Modeling of the MB adsorption onto GCB

The Langmuir model hypothesizes that the adsorption occurs at specific sites of the absorbent, with no further adsorption on the occupied binding site. The linearized form of Langmuir model is given below:

$$\frac{1}{q_e} = \frac{1}{Q_M} + \left(\frac{1}{Q_M K_L}\right)\frac{1}{C_e} \tag{5}$$

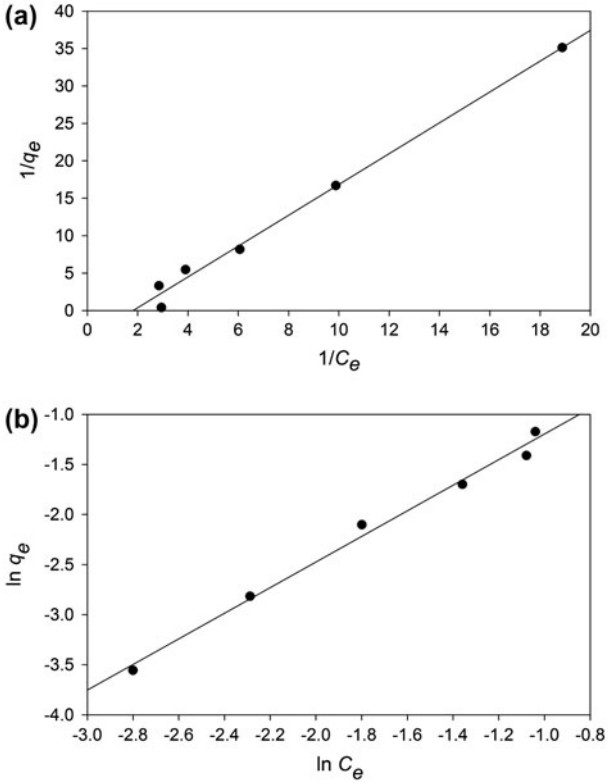

Fig. 4. Linearization plots of adsorption isotherm model for the adsorption MB on GCB: (a) Langmuir model; (b) Freundlich.

where Langmuir constant (Q_M and K_L) can be calculated from the plot of $1/q_e$ as the function of $1/C_e$ which intercept (*c*) and linear slope (*m*) in the linear equation correspond to $1/Q_M$ and $1/Q_MK_L$, respectively.

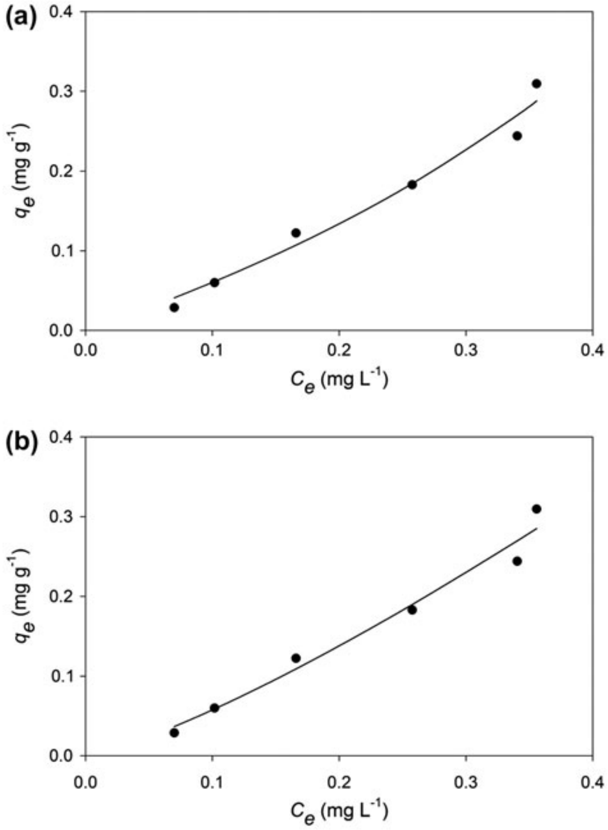

Fig. 5. Non-linear curve fitting of experimental data (a) Langmuir model; (b) Freundlich isotherms.

The derivation of Freundlich model is based on the assumption that heterogeneous surface is caused by the different distributions of the energy on

Table 5
Estimation of Langmuir and Freundlich constant using (a) linearization method and (b) non-linear regression

(a)

Langmuir Model		Freundlich Model		
Q_M	K_L	$1/n$	n	K_F
−0.2639	−0.5433	1.2783	0.7823	1.0858

(b)

	Langmuir Model		Freundlich Model	
Model constants	Q_M	K_L	n	K_F
Initial guess[a]	−0.2639	−0.5433	0.7823	1.0858
Estimated	−0.6004(1.0228)	−0.9111(1.0951)	0.7922(0.2778)	1.0506(0.5633)

Note: 95% confidence interval.

[a] Initial guess was determined from linearization plot.

Table 6
Post-modeling statistics for Freundlich isotherm

Freundlich isotherm	R^2	R^2 adjusted	Variance
Linearization	0.9908	0.9885	0.0095
Non-linear regression	0.9735	0.9669	0.0003

absorbent surface. The linear form of the Freundlich equation can be written as follows:

$$\ln q_e = \ln K_F + \frac{1}{n} \ln C_e \tag{6}$$

where the slope of linear plot and the y-intercept represents the value for $1/n$ and ln K_F, respectively. The linearization results of Langmuir and Freundlich models and their estimated constants are shown in Fig. 4 and Table 5(a), respectively. The negative value for Langmuir constant from the linearization of a data point is not representative of the actual behavior of Langmuir model.

To verify the estimated constants, the constant values were also calculated using non-linear regression method. The non-linear equation for Langmuir (Eq. (3)) and Freundlich (Eq. (4)) was used to fit the experimental data (Fig. 5). The regression analysis was performed using Polymath 6.0 software with Levenberg–Marquardt (LM) algorithm (Table 5(b)). The large value of 95% confidence interval (CI) for Langmuir constant estimated using non-linear regression method suggested the model was unstable resulted in large changes of parameter values with small change in the data point. On the other hand, the 95% CI of Freundlich model was much smaller than the estimated constant values.

Since the negative constant value of Langmuir model does not represent the actual adsorption behavior, the model was not considered further for modeling of MB adsorption onto GCB. The statistical analysis for modeling of experimental data is summarized in Table 6. The correlation coefficients (R^2 and R^2 adjusted) and variance showed the linearization and non-linear regression of Freundlich model adequately fitted the experimental data.

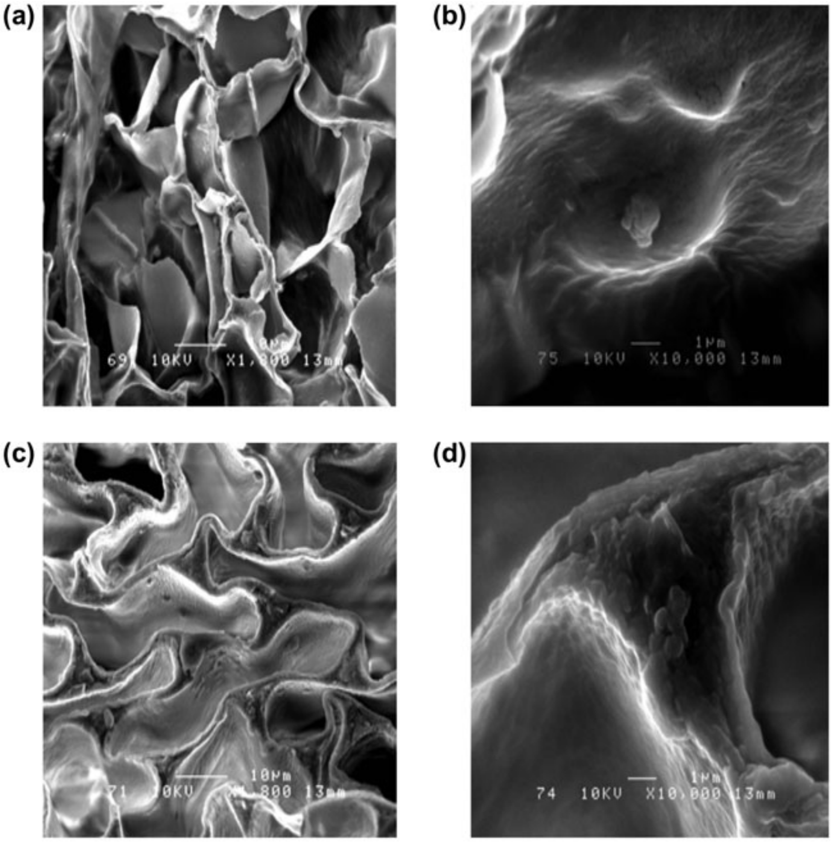

Fig. 6. SEM of GCB: (a) magnification × 1,800 (before treatment); (b) magnification × 10,000 (before treatment); (c) magnification × 1,800 (after treatment); and (d) magnification × 10,000 (after treatment).

From SEM micrographs (Fig. 6), it can be observed that the surface of GCB is made up by a porous structure on which dye molecules may be adsorbed on the surface as well as on the active centers within the pores of the grated copra fibers. This assumption was supported by the adsorption isotherm analysis where the adsorption of MB on GCB is adequately explained by the Freundlich adsorption model.

4. Conclusion

The optimum dye decolorization of 80–85% decolorization was obtained using GCB at 0.75 g and initial dye concentration at 8 μg mL^{-1}. It is hypothesized that the dye is adsorbed throughout the mass of GCB. This is strongly supported by the porous structure of the copra as shown in SEM. From this study, GCB is potentially utilized as an alternative low-cost and green biosorbent for dye removal in aqueous environment.

Acknowledgments

This research was supported by grant No. UMRG048-11BIO and PV016-2011B, University of Malaya Kuala Lumpur, Malaysia.

References

[1] S.P. Raghuvanshi, R. Singh, C.P. Kaushik, Kinetics study of methylene blue dye bioadsorption on bagasse, Appl. Ecol. Environ. Res. 2 (2004) 35–43.

[2] H.W. Chih, F.P. Yi, Adsorption of a cationic dye (methylene blue) onto spent activated clay, J. Hazard. Mater. 144(1–2) (2007) 355–362, doi: 10.1016/j.jhazmat.2006.09.097.

[3] J. Song, W. Zou, Y. Bian, F. Su, R. Han, Adsorption characteristics of methylene blue by peanut husk in batch and column modes, Desalination 264(1–3) (2011) 119–125, doi: 10.1016/j.desal.2010.07.041.

[4] H. Xiuli, W. Wei, M. Xiaojian, Adsorption characteristics of methylene blue onto low cost biomass material lotus leaf, Chem. Eng. J. 171(1) (2011) 1–8, doi: 10.1016/j.cej.2011.02.067.

[5] K.S. Low, C.K. Lee, The removal of cationic dyes using coconut husk as an adsorbent, Pertanika 13(2) (1990) 221–228.

[6] M.A. Ashraf, I. Yusoff, I. Yusof, Y. Alias, Study of contaminant transport at an open tipping waste disposal site, Environ. Sci. Pollut. Res. 20(7) (2013) 4689–4710, doi: 10.1007/s11356-012-1423-x.

[7] A.F. Abu Bakar, I. Yusoff, Ng. Tham Fatt, F. Othman, M.A. Ashraf, Arsenic, zinc, and aluminium removal from gold mine wastewater effluents and accumulation by submerged aquatic plants (*Cabomba piauhyensis*, *Egeria densa*, and *Hydrilla verticillata*), BioMed Res. Int. 2013 (2013) 7, doi: 10.1155/2013/890803.

[8] H.W. Chih, T.L. Yao, W.T. Tai, Removal of methylene blue from aqueous solution by adsorption onto pineapple leaf powder, J. Hazard. Mater. 170(1) (2009) 417–424, doi: 10.1016/j.jhazmat.2009.04.080.

[9] D.C. Creswell, C.C. Brooks, Composition, apparent digestibility and energy evaluation of coconut oil and coconut meal, J. Anim. Sci. 33(2) (1971) 366–369.

[10] AOAC. International Method 973.18, fiber (acid detergent) and lignin in animal feed, in: Official methods of analysis of AOAC international, sixteenth ed., Arlington, VA, 1997, pp. 28–29, doi: 10.1016/j.desal.2008.09.012.

[11] S.T. Akar, A.S. Ozcan, T. Akar, A. Ozcan, A. Kaynak, Biosorption of a reactive textile dye from aqueous solutions utilizing an agro-waste, Desalination 249(2) (2009) 757–761.